Available online at www.sciencedirect.com
SCIENCE DIRECT®
C. R. Physique 6 (2005) 966–976
COMPTES RENDUS PHYSIQUE
http://france.elsevier.com/direct/COMREN/

Spintronics/Spintronique

Spintronic with semiconductors

Jean-Marie George [a,*], Marc Elsen [a], V. Garcia [a,b], Henri Jaffrès [a], Richard Mattana [a]

[a] *Unité Mixte de Physique CNRS/Thales, route départementale 128, 91676 Palaiseau cedex, France and Université Paris-Sud, 91405 Orsay, France*
[b] *Institut des NanoSciences de Paris, universités Paris 6 et Paris 7, CNRS UMR 7588, 140, rue de Lourmel, 75015 Paris, France*

Available online 5 December 2005

Abstract

Soon afterwards the discovery of the giant magnetoresistance in metallic multilayers, researchers have attempted to integrate spintronic properties with semiconductor materials. They came up against several difficulties related to the structural and electronic properties of the ferromagnetic metal-semiconductor interface. We will report on the recent progress made in this field of spintronic with semiconductors. First of all we will explain the interfacial resistance conditions required to inject and detect efficient spin current in a semiconductor and in a second part we will show that efficient spin injection experiments have been now achieved thanks to the addition of a tunnel resistance at the interface. We will then report on the magnetoresistance experiment performed with diluted magnetic semiconductors as ferromagnetic material. This type of material can constitute an alternative road to achieving electrical control spintronic devices. Finally, we will finish by reporting on research for a highly spin-polarized source to inject spin-polarized current in a semiconductor. It will be mainly focused on tunnel magnetoresistance junctions with semiconductor barriers and hot electron transistor. ***To cite this article: J.-M. George et al., C. R. Physique 6 (2005).***

Résumé

Électronique de spin avec semiconducteurs. Peu après la découverte de la magnétorésistance géante dans des multicouches métalliques, les chercheurs ont essayé d'intégrer les propriétés de l'électronique de spin avec celles des semiconducteurs. Les difficultés rencontrées sont liées aux propriétés structurales et électroniques de l'interface métal-semiconducteur. Plus récemment des avancés significatives ont été réalisées. Nous décrirons les progrès récents réalisés dans ce domaine de l'électronique de spin avec semiconducteurs. Dans un premier temps nous montrerons quelles sont les conditions requises afin d'injecter et de détecter efficacement un courant de spin dans un semiconducteur. Ces conditions peuvent être déduites de considérations théoriques. Nous montrerons qu'une injection électrique de spins peut être obtenue grâce à l'insertion d'une résistance d'interface entre le métal ferromagnétique et le semiconducteur. Ensuite nous décrirons des expériences de magnétorésistance réalisées avec un semiconducteur magnétique dilué comme matériau ferromagnétique. Ce type de matériaux peut constituer une alternative pour réaliser des dispositifs d'électronique de spin contrôlés électriquement. Enfin nous décrirons les recherches effectuées sur les sources de courant fortement polarisées en spin. Nous nous limiterons aux jonctions tunnel magnétiques dont les barrières sont composées de semiconducteurs et au transistor d'électrons chauds. ***Pour citer cet article : J.-M. George et al., C. R. Physique 6 (2005).***

Keywords: Spintronic; Ferromagnetism; Semiconductors

* Corresponding author.
E-mail address: jean-marie.george@thalesgroup.com (J.-M. George).

1631-0705/$ – see front matter © 2005 Académie des sciences. Published by Elsevier SAS. All rights reserved.
doi:10.1016/j.crhy.2005.10.009

Mots-clés : Electronique de spin ; Ferromagnétisme ; Semiconducteurs

1. Introduction

Spintronics is a multidisciplinary field whose central concept is the active manipulation of the spin degree of freedom in solid state systems. The potentiality of controlling spin currents was first demonstrated in metallic structures with the discovery of the Giant Magnetoresistance (GMR) [1], and related applications in the field of magnetic sensors and read heads [2]. These metallic structures are based on ferromagnetic metals in which, as first suggested by Mott [3,4], the electrical current is carried by independent majority and minority spin channels [5]. In other words, a ferromagnetic metal is naturally a spin-polarized conductor. Soon after the discovery of GMR, the interest of combining the charge manipulation of conventional electronics with the spin manipulation of spintronics was rapidly understood. The advantages expected are the non volatility of the spin information, the integration of new functionality, the powerless consumption, etc., [6]. In 1990, Data and Das first proposed the concept of spin Field Effect Transistor (spin FET) [7] which has driven many experiments. Unfortunately, the results were disappointing and, today, two main reasons can be put forward to explain the difficulties encountered. The first comes from the difficulty of growing a ferromagnetic transition metal with semiconductor materials. This led to a large number of structural and chemical interfacial studies. The second is more fundamental, and was only pointed out and debated after the year 2000. Due to the large difference in density of states between a metal and a semiconductor (conductivity mismatch), most of the spin relaxation occurs in the metal in the absence of interfacial resistance.

During the last few years, noticeable results have been obtained in the field of spintronics with semiconductors, which have boosted the research. We will report here on 3 important achievements that conduct the organization of this article. The first, as previously mentioned, is the theoretical understanding of the injection and detection conditions needed to generate a spin current in a semiconductor. They will be explained in Section 2. The second, closely related to the injection condition, is the experimental demonstration of efficient spin-polarized current injection and transport in a semiconductor. The basis of the experiment, which involves optical detection of polarized light, will be described. Thanks to this set of experiments, we identify interfacial combinations of efficient spin injectors, which constitute the first step to the fabrication of a complete solid electrical device. Third, another important step was the discovery of III–V ferromagnetic semiconductors [8,9]. The most well-known and well characterized is the $Ga_{1-x}Mn_xAs$. This so-called diluted magnetic semiconductor (DMS) can constitute an alternative to the use of ferromagnetic transition metals and has the advantage of a better integration in a semiconductor structure. Even if there is not yet clearly established room temperature ferromagnetic semiconductors, the study of GaMnAs heterostructures brings new insight in the field of spintronics with semiconductors. It will constitute Section 4. Finally before the conclusion, we will finish, as Section 5, with some new developments in the field. This will mainly focus on the research of new highly polarized spin injectors. For a more detailed review, including spin relaxation mechanisms, we refer the reader to Zutic et al. [10].

2. Theory

2.1. General trends for ferromagnetic metal/semiconductor structures

The spin injection problem is typically a problem of spin transport through an interface between a ferromagnetic conductor and non-magnetic one. The difficulty of spin injection when the ferromagnetic conductor is a metal, has been first put forward by Schmidt et al. [11]. As has been shown by Rashba [12] and Fert and Jaffrès [13], spin injection from a ferromagnetic metal can be achieved only by introducing a large enough interface resistance, typically a tunnel junction. Spin injection through a single interface is involved in Spin-LED (spin Light Emitting Diode) experiments and spin injection from a ferromagnetic metal through a tunnel barrier or in the tunneling regime of a Schottky junction has been now clearly demonstrated for spin LED (cf. Section 3). In a structure with ferromagnetic source and drain, both the source/semiconductor and semiconductor/drain interfaces are similarly involved in the problem of spin injection, and spin-dependent interface resistance must be inserted at both places.

The spin conservation problem is specific to the source/semiconductor/drain structure (two interfaces) and related to the contrast between the conductance of the parallel (PA) and antiparallel (AP) magnetic configurations of the structure (parallel/antiparallel meaning with parallel/opposite orientations of the source and drain magnetization). More quantitatively, if we call V the voltage between source and drain and ΔV the excess voltage in the AP state for the same current, we want $\Delta V/V$ to be of the order of the spin polarization of the injected electrons, that is, typically of the order of unity. Actually, the condition for $\Delta V/V \approx 1$ is twofold. First, there must be injection of a spin-polarized current which requires a spin-dependent and large enough resistance at both the source/semiconductor and semiconductor/drain interfaces (left branch of Fig. 1). Secondly, there

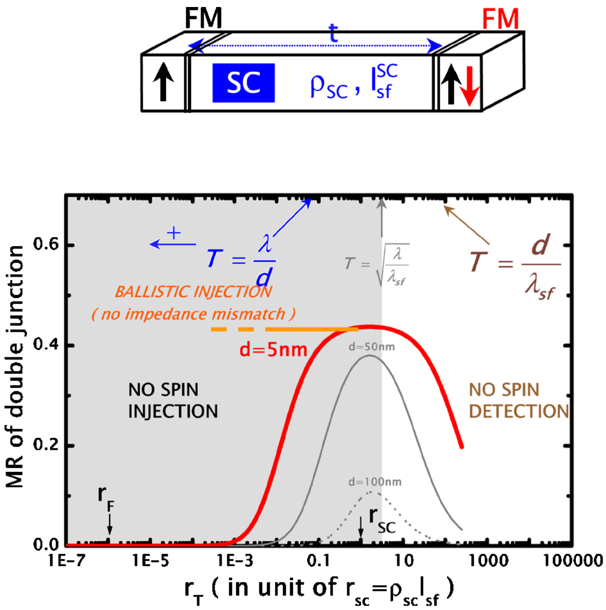

Fig. 1. Plot of the magnetoresistance of FM//SC//FM structure in vertical geometry (upper structure) expected versus the value of the spin-dependent interface resistance (lower scale) or spin-dependent interface transparency (upper scale). The left branch corresponds to the condition of spin injection, whereas the right one corresponds to the condition of spin conservation within the semiconductor. The scale of resistance is given taking into account data for GaAs from Ref. [40].

must be a strong contrast between the spin accumulations in the PA and AP states; this we call the spin accumulation condition. More precisely, the spin accumulation relaxation rate in the semiconductor must be much slower than the spin injection rate. As we will see, this can occur if the interface resistance is smaller than a certain threshold value [13] (right branch of Fig. 1).

In summary, to obtain an optimum contrast between the conductance of the PA and AP states, which requires spin polarization of the current (at least in the PA state) and conservation of the spin accumulation (at least in the AP state), two conditions must be fulfilled:

- a spin-dependent interface resistance must be introduced between the semiconductor and the metallic source and drain;
- the value of the interface resistances must be chosen in a well defined window (see characteristic curve in Fig. 1).

This window shrinks and disappears when the spin diffusion length (SDL) becomes shorter than the length of the semiconductor channel (in contrast with what has been sometimes proposed, a SDL longer than the semiconductor channel is not a sufficient condition). The lower edge of the window corresponds to the condition for spin injection. This condition exists when the conductivity is larger, or the spin lifetime shorter, in the source and drain, that is typically the case for metallic magnetic materials. The upper edge of the window corresponds to the condition for spin conservation (larger spin accumulation in the AP state) and optimum $\Delta V/V$. As it will be put forward below, the condition associate to the upper edge of the window in Fig. 1 can also be described as the condition of a long spin lifetime (τ_{sf}) compared to the particle dwell time (τ_n or equivalently their characteristic injection time and ejection time) in the semiconductor channel between its injection from the source and its ejection towards the drain. This condition of spin conservation exists for any type of magnetic material, metal or semiconductor. An experimental demonstration of this condition for source and drain made of the semiconductor GaMnAs is presented in Section 4 of this article. What has been written above is implicit for diffusive transport in the semiconductor. For ballistic transport, as we will see in detail in the following part, the condition for spin conservation and optimum ΔV (the upper edge of the window) still exists.

2.2. Spin injection, spin conservation and magnetoresistance in FM/SC/FM structures

2.2.1. Definition and physical parameters

We consider two identical ferromagnetic (FM) contacts, L (left) and R (right), connected along the z direction by a semiconductor (SC) whose geometry is characterized by a channel length t and a section S (relative to the contact area, taken to be equal to unity). In the following we will neglect the effect of the electrical field (drift current) which is almost valid in the limit of the low bias. This effect can be take into account and lead to an asymmetry of the length or time scale of the injection–detection problem [14].

The one-dimensional (1-D) density of states (DOS) in SC and FM along z is noted ρ_{SC} and $\rho_{FM\pm}$ respectively, where the subscript $+$ $(-)$ refers to up (down) spins, respectively. Interfaces between FM (L or R) and SC, assumed to be identical, are characterized by (i) a spin-dependent flux transmission, $T_\pm = T(1 \pm P)$ with the result that the tunnel polarization at the Fermi level can be written $P = (T_+ - T_-)/(T_+ + T_-)$, equivalent to the Jullière definition [15]; and by (ii) the number, n_{2D}, of two-dimensional (2-D) channels in SC connected to FM as appearing in the Landauer formula [16]. For a non-magnetic semiconductor, these number of channels are equal for both spin populations.

From the Hamiltonian transfer approach [17], we can express for a particle (i) its characteristic time of injection from FM (L or R) towards into SC, $\tau_{FM\to SC}$; (ii) its spin-dependent time of ejection, $\tau_\pm$, from SC into FM (L or R); and (iii) its spin-dependent transmission ($T_\pm$). Corresponding currents ($J_{FM\pm\to SC}$) and conductivity ($G_{FM\pm\to SC}$) for a given interfacial channel follow, according to:

$$\begin{aligned}
\Gamma_{FM} &= \frac{\hbar}{\tau_{FM\to SC}} = 2\pi \left|\langle \phi^Z_{FM}|H_T|\phi^Z_{SC}\rangle\right|^2 \rho_{sc}\\
\Gamma_{SC} &= \frac{\hbar}{\tau_\pm} = 2\pi \left|\langle \phi^Z_{FM}|H_T|\phi^Z_{SC}\rangle\right|^2 \rho_{FM\pm}\\
T_\pm &= (2\pi)^2 \left|\langle \phi^Z_{FM}|H_T|\phi^Z_{SC}\rangle\right|^2 \rho_{sc}\rho_{FM\pm}\\
J_{FM\pm\to SC} &= \frac{e}{\hbar}\int 2\pi \left|\langle \phi^Z_{FM}|H_T|\phi^Z_{SC}\rangle\right|^2 \rho_{sc}\rho_{FM\pm}\, d\varepsilon_{FM,SC}\\
G_{FM\pm\to SC} &= e\frac{\partial J_{FM\pm\to SC}}{\partial \varepsilon_{FM,SC}} = \frac{e^2}{h} T_\pm
\end{aligned} \tag{1}$$

where ϕ_{FM} and ϕ_{SC} are the normalized one-dimensional wave functions in FM and SC connected through the interface by the transfer Hamiltonian H_T. Γ_{FM} and Γ_{SC} represent the broadening of the energy level in FM (ε_{FM}) and SC (ε_{SC}) introduced by the leak towards FM (L or R) and SC. Note that the spin-polarized current $J_{FM\pm\to SC}$ crossing each surface (L/SC or SC/R) per unit time and per unit number of 2-D channels does not depend on the propagation direction.

2.2.2. Magnetoresistance

By expressing the escape time $\tau_\pm$ as a function of the 1-D DOS, ρ_{SC}, and the spin-dependent transmission at interfaces (T) one can derive a simple expression for the magnetoresistance, a function of the spin life time and the escape time [18].

The term $MR = J_{PA}/J_{AP} - 1$ can be expressed:

$$MR = \frac{[\tau_- - \tau_+]^2}{4(\tau_-\tau_+)} \frac{1}{1 + (\tau_+ + \tau_-)/(2\tau_{sf})} \tag{2}$$

2.2.3. Condition for impedance matching without spin relaxation

Neglecting the spin relaxation in SC ($\tau_{df} = \infty$), the MR equals $(\tau_- - \tau_+)^2/4\tau_-\tau_+$ which can be expressed versus the effective transmission coefficients at interfaces, $T_{*\pm}$, according to $MR = (T_{*+} - T_{*-})^2/(4T_{*+}T_{*-})$. From the upper relation $[T_{*\pm}]^{-1} = [T_\pm]^{-1} + [T_{*SC}]^{-1}$ with $T_{*SC} = \lambda/(t - \lambda)$, one can express the MR versus the unpolarized intrinsic transmission T as $MR = \kappa P^2/(1 - P^2)$ with $\kappa = 1/[1 + 2T/T_{SC} + (1 - P^2)(T/T_{SC})^2]$. The maximum MR for symmetric double tunnel junction is then $P^2/(1 - P^2)$, that is, half of TMR of single junctions. The factor $1/2$ is related to accumulation effects in the central non-magnetic electrode. Starting from this optimal value, the MR decreases when $\kappa < 1$ or $T > T_{*SC}$, that is when the impedance matching is incomplete [11,13] for interface transparencies larger than the transmission through the SC channel. Note that this impedance mismatch is also associated with a vanishing current spin-polarization in the PA state. The introduction of tunnel junctions of small transmission $T \ll T_{*SC} = \lambda/(t-\lambda)$ (or high resistive enough) at the interfaces restores the current spin-polarization in PA state and consequently the MR [12,13]. For a diffusive transport in SC ($t \gg \lambda$), the condition $T_L < \lambda/t$ is equivalent to $T_L < \sqrt{\tau_p/\tau_{LR}}$ where τ_p and τ_{SC} represents respectively the momentum relaxation time (τ_p) and the characteristic time (τ_{LR}) for a particle to diffuse from the left to the right interface in SC. $1/\sqrt{\tau_p/\tau_{SC}}$ represents the number of reflections of a particle upon the left interface once injected in SC and before being detected in R after a delay time τ_{SC}. The condition of impedance matching is then the condition for a spin to be detected in the R contact instead of diffusing back towards the emitter L (where its spin will be rapidly lost).

2.2.4. Condition for spin conservation with impedance matching

The second term appearing in the expression of MR, that is $[1 + (\tau_+ + \tau_-)/2\tau_{sf}]^{-1}$, represents a reduction factor related to the condition of spin conservation in the SC channel once the impedance matching is completed. To obtain any MR effects,

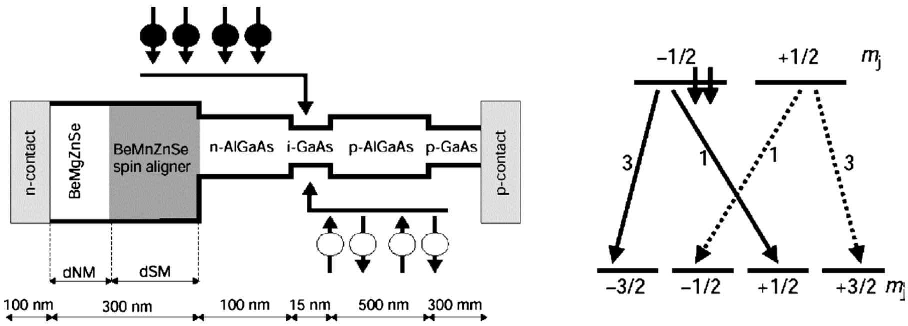

Fig. 2. Band structure of the spin-LED. Spin-polarized electrons are injected from the paramagnetic semiconductor into AlGaAs (left). Selection rules for GaAs; recombination between electrons and heavy holes is three times larger than recombination between electrons and light holes. From Fiederling et al. [20].

the spin lifetime in SC must be larger than the mean dwell time of $+$ and $-$ spins in the SC channel (in the PA state). This mean dwell time is noted there τ_n and equals $(\tau_+ + \tau_-)/4$. The loss of spin memory in SC originates from the large number of reflections at the two interfaces. This effect can be viewed as the consequence of a too large integrated ballistic path in SC compared to the spin mean free path l_{sf}. Indeed, from the developments above, the condition for spin conservation in SC reads $T > h\rho_{SC}/\tau_{sf} \approx t/\lambda_{sf}$ or $l = t/T < \lambda_{sf}$ where l represents the integrated particle path in both ballistic ($t < \lambda$) or diffusive ($t > \lambda$) regimes of injection.

As a conclusion, the conditions acting on the interface transparency (T) between FM and SC to obtain MR in the FM/SC/FM junction, that is, an electrical injection and detection of spins, are $t/\lambda_{sf} < T < \lambda/t$ in current-perpendicular to plane experiments (or heterostructure of constant section) and more generally $S[t/\lambda_{sf}] < T < S[\lambda/t]$ for a lateral spin transport where S is the ratio of the SC section to the contact section (refer to geometric effects in [13]).

3. Demonstration of electrical spin injection efficiency: Spin-LED experiments

One way to probe electrical spin injection in a semiconductor is the use of a light emitting diode as a spin detector. In a quantum well and in Faraday geometry the electron-hole recombination in a quantum well gives rise to a circular polarized photon [19]. Taking into account the spin polarization at the interface FM/NM, the spin relaxation mechanisms in the SC and in the QW, electrical spin injection efficiency can be estimated from the degree of circular polarization of the photons emitted by the light emitting diode. Fig. 2 gives a schematic picture of the selection rules for circular polarized emission in the case of a degenerate valence band for heavy and light holes in the quantum well.

Electrical spin injection has first been reported in 1999 by Fiederling et al. [20]. In this experiment, Fiederling et al. used a paramagnetic semiconductor as spin injector. Magnetic semiconductors present the advantage of being free from conductivity mismatch and chemical reactivity problems. Furthermore, paramagnetic semiconductors are fully spin-polarized at low temperatures and at high magnetic fields. Since this preliminary result, many experiments have been reported using similar or other magnetic materials (ferromagnetic semiconductor, transition metals and ferromagnetic metals) and other interface resistance (Schottky barrier, tunnel barrier). Major results are summarized in Table 1. Because the technique requires the emission of photons, most of the experiments were performed in $Ga_{1-x}Al_xAs$ materials with GaAs or InAs QW or Q. We can point out that with a transition metal, the higher polarization injected was obtained in a tunnel regime with CoFe/MgO/GaAs interface. This provides also an experimental confirmation of the necessity of adding an interfacial resistance (Schottky or Tunnel) to inject efficient spin-polarized current in a semiconductor, as developed in previous section.

4. Magnetic semiconductors

Another important result has been the discovery of ferromagnetic semiconductors. As already discussed previously, the use of transition metals to electrically inject spins in semiconductors is faced with two drawbacks: the chemical reactivity between metals and semiconductors and the so-called ‘conductivity mismatch’. One way to avoid these two difficulties is the use of ferromagnetic semiconductors as spin injector and spin analyzer. Indeed ferromagnetic semiconductors and non-magnetic semiconductors have more compatible growth conditions as well as closer density of states and conductivity.

Table 1
Major results of electrical spin injection with an optical detection. Magnetic materials, type of resistance, LED structure and optical polarization of light emitted are listed. The value of the associated spin polarization can be found in the original reference

Magnetic material	Interface resistance	Semiconductor structures	Optical polarization (%)	Reference
BeMnZnSe	Ohmic contact	AlGaAs/GaAs/AlGaAs quantum well	45	[20]
ZnMnSe	Ohmic contact	AlGaAs/GaAs/AlGaAs quantum well	50	[21]
Fe	Schottky barrier	AlGaAs/GaAs/AlGaAs quantum well	32	[22]
Fe	Schottky barrier	GaAs/InGaAs/GaAs quantum well	2	[23]
Co	Schottky barrier	AlGaAs/GaAs/AlGaAs quantum well	4	[24]
Co_2MnGe	Schottky barrier	AlGaAs/GaAs/AlGaAs quantum well	13	[25]
MnAs	Schottky barrier	GaAs/InGaAs/GaAs quantum well	1	[26]
CoFe	Al_2O_3 Tunnel barrier	AlGaAs/GaAs/AlGaAs quantum well	21	[27]
CoFe	MgO Tunnel barrier	AlGaAs/GaAs/AlGaAs quantum well	57	[28]
GaMnAs	Zener diode: GaMnAs/GaAs n+	AlGaAs/GaAs/AlGaAs quantum well	20	[29]
BeMnZnSe	Ohmic contact	ZnSe/CdSe/ZnSe quantum dots	70	[30]
Fe	Schottky barrier	GaAs/InAs/GaAs quantum dots	5	[31]

4.1. Origin of ferromagnetism

If the origin of the ferromagnetic phase is well established for most of semiconductors ($Ga_{1-x}Mn_xAs$ [9], $In_{1-x}Mn_xAs$ [8], $Zn_{1-x}Mn_xTe$ [32], $Cd_{1-x}Mn_xTe$ [33], Mn_xGe_{1-x}) [34], it is still debated for other semiconductors such as $Ga_{1-x}Mn_xN$ [35] or $Zn_{1-x}Co_xO$ [36]. In this review, we focus on the well-known $Ga_{1-x}Mn_xAs$ ferromagnetic semiconductors. Ferromagnetic semiconductors can be considered as composed of two coupled electronic systems, one containing delocalized electrons (conduction or valence band) and another containing the electrons of magnetic impurities with a localized magnetic moment. There is (i) magnetic interactions between the delocalized carriers and electrons of magnetic impurities; and (ii) interactions between magnetic ions.

(i) The interaction s(p)-d between delocalized carriers and electrons of magnetic impurities is ferromagnetic in the case of itinerant electrons and antiferromagnetic for holes. The exchange constant α (s-d) or β (p-d) is generally greater for holes, thus an antiferromagnetic coupling between holes and magnetic impurities occurs.

(ii) The magnetic interaction between magnetic ions can be dealt with RKKY and Zener mechanisms in the case where the magnetic ion concentration is larger than the carrier concentration. Spin-orbit and carrier–carrier interactions are difficult to take into account in the RKKY model. Therefore the Zener model is used to describe the magnetic properties of ferromagnetic semiconductors [37]. In heavily doped ferromagnetic semiconductors ($x > 3\%$), the mean distance between carriers ($r_c = 4/3\pi p)^{-1/3}$ is much longer than the distance between magnetic ions ($r_s = 4/3\pi x N_0)^{-1/3}$. The first zero of the RKKY interaction is equal to $r \sim 1.17 r_c$, thus the interaction induced by carriers is ferromagnetic and long range. The exchange integral $N_0\beta$ is larger than $N_0\alpha$, the ferromagnetic phase is favored in p-type semiconductors. In this way, delocalized holes are necessary to obtain a ferromagnetic phase in semiconductors doped with magnetic ions.

Because the magnetic properties depend on the itinerant carrier concentration (holes), a variation of the carrier density induces a modification of the magnetic properties. For instance, several studies (in Mn doped InAs [38], Ge [34] or CdTe quantum wells [39]) have shown that the Curie temperature can be tuned by an electric field or by light. These experiments well demonstrate the interplay between carriers and magnetic ions.

According to growth conditions (growth temperature, As_4/Ga beam equivalent pressures ratio), $Ga_{1-x}Mn_xAs$ layers are conductors (about mΩ cm) and ferromagnetic with a Curie temperature about 150 K for a Mn concentration between 3% and 7%. Outside this range, layers are insulating or contain MnAs clusters [40].

Both diluted magnetic semiconductors and ferromagnetic semiconductors have been inserted in semiconductor heterostructures. Ferromagnetic semiconductors, $Ga_{1-x}Mn_xAs$ in particular, have been used in various heterostructures. For instance, one can note experiments on spin-dependent tunneling in tunnel junctions [41], electrical detection of spin accumulation in semiconductor quantum wells [42], current induced magnetic switching in magnetic tunnel junctions [43] or electrical spin injection in light-emitting diodes [29].

4.2. Magnetic tunnel junctions

To probe the spin-polarization of holes tunneling from GaMnAs through III–V tunnel barriers, studies have been performed on GaMnAs/AlAs/GaMnAs magnetic tunnel junctions. The structures have been elaborated at 230 °C on a GaAs buffer layer grown at 580 °C. Thin layers of 1 nm GaAs layer have been inserted at each side of AlAs to prevent Mn diffusion into the barrier [44]. M(H) hysteresis loops of the stack measured before patterning show two steps associated to a separate reversal of

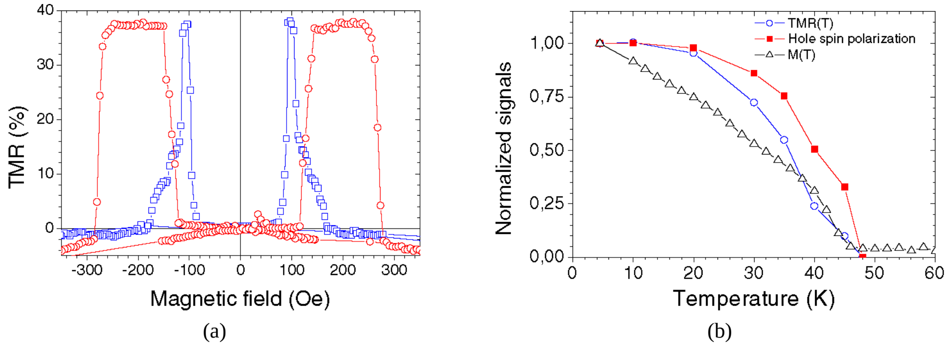

Fig. 3. Tunnel magnetoresistance of single (circles) and double (squares) tunnel junctions recorded at 4 K and 1 mV. Temperature dependence of magnetization, TMR and spin hole polarization deduced from Jullière model of the single MTJ.

the two GaMnAs layers. Nevertheless, we have not annealed our junctions to avoid possible Mn diffusion. Fig. 3 displays the tunnel magnetoresistance (TMR) measured at low bias (1 mV) and low temperature (4.2 K). The TMR, that is a probe of hole spin polarization, is nearly as high (40%) as for the junctions of [41] with the same AlAs thickness. Using the simple Jullière formula [15], $TMR = 2P^2/(1 - P^2)$, a tunnel polarization of 40% for holes can be derived from these experiments even if its microscopic understanding still remains a difficult task [46]. Fig. 3 compares the variation of the hole tunnel spin polarization versus T deduced from our transport measurement to that of the magnetization obtained by a SQUID magnetometer before patterning. Although both quantities cancel at the GaMnAs Curie temperature, the characteristic shapes are clearly different, the hole polarization saturating at higher T. Such different magnetic susceptibility between holes and Mn localized de moments can be explained by a stronger effective field experienced by the holes [37]. Nevertheless, microscopic calculations of the spin-polarized tunneling in GaMnAs/AlAs/GaMnAs structures are urgently required to allow a definite conclusion.

Note that other spin-dependent tunneling experiments on junctions with (Al,Ga)As, (In,Ga)As and GaAs tunnel barrier have been performed. At very low temperature and low bias voltage, TMR reaches 300% [47]. Recently, tunneling anisotropic magnetoresistance has been discovered [48]. This effect is the signature of the anisotropy of the valence band in GaMnAs.

4.3. Electrical spin injection and detection into GaAs quantum wells

As developed in Section 2, the occurrence of TMR on double tunnel junctions is the signature of a spin accumulation in the central semiconductor layer. To illustrate this idea, we have grown double tunnel junctions still constituted of two GaMnAs electrodes and where a thin GaAs layer (3, 5, 6 and 9 nm) has been inserted in between two AlAs barriers leading to GaMnAs/AlAs/GaAs/AlAs/GaMnAs structures. The thickness of the AlAs barrier lies between 1.46 to 1.95 nm. Auger nanoscale spectroscopy studies confirm that the insertion of a thin 1 nm GaAs layer between GaMnAs and AlAs is sufficient to prevent any Mn diffusion into the GaAs QWs (Mn concentration less than 0.1%). A large TMR effect of about 40% is observed at low temperature (Fig. 4(a)). As described in [42], the TMR of our double junctions cannot be explained by a direct coherent tunneling between the GaMnAs electrodes, but must be described by sequential tunneling with spin conservation in the GaAs QWs. This has to be associated to the half of the TMR of single junction with 1.46 nm AlAs barrier from [41]. In FM/NM/FM structure and in the antiparallel magnetic configuration, spin accumulation takes place in the non-magnetic layer if the number of spins injected is larger than the number of spin-flips. In our structures, tunnel magnetoresistance associated with this spin accumulation in the quantum well, reflects a hole spin lifetime longer than the dwell time of holes in the quantum well. To probe this condition, we have played independently with these two characteristic times.

On Fig. 4(a), we have reported the TMR recorded at 4 K on different 6 nm QWs as a function of their resistance-area product RA. The resistance variation is attributed to the change of the barrier thickness from 1.46 to 1.95 nm as demonstrated by Transmission Electronic Microscopy (TEM) on cross-sections. What we observe is a continuous decrease of TMR versus RA related to the reduction of the tunnel transmission. As fitted by the dotted line in Fig. 4, this behavior must be ascribed to the rise of the particle dwell time τ_n in GaAs beyond its spin lifetime τ_{sf} in GaAs for the largest barrier thickness [18]. Another way to test this condition is to play with the spin lifetime. An increase of temperature is associated to some activation of spin-flip mechanisms in quantum wells and therefore a strong shortening of the spin lifetime. At 15 K, well below the Curie temperature, the hole spin lifetime becomes shorter than the dwell time and therefore TMR vanished [49]. By estimating the dwell time and using Eq. (2), we can estimate the spin life time of the holes at 100 ps. A so long spin life time for holes can be understood by supposing a tunneling mechanism via extended defects in the quantum well [42]. Moreover, this represents an experimental test of the upper resistance condition (cf. Section 2).

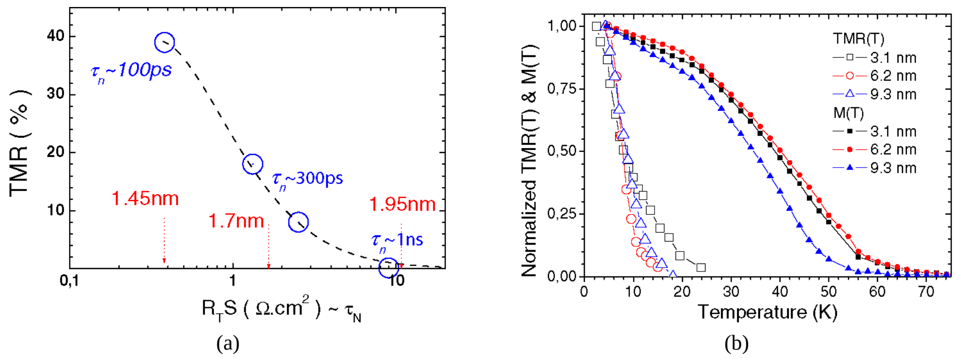

Fig. 4. Dependence of TMR with the resistance of AlAs tunnel barriers for 6.2 nm GaAs QW width and dependence of TMR and magnetization with temperature for different GaAs thickness. An increase of AlAs resistance tunnel results an increase of dwell time and therefore a decrease of TMR. As temperature increases, hole spin lifetime decreases and becomes shorter than the dwell time, thus TMR vanishes well below the Curie temperature.

5. Research of highly spin-polarized source

Following the pioneering work of Jullière [15], the discovery of large tunneling magnetoresistance effects (TMR) at room temperature with magnetic tunnel junctions (MTJs) [45] offers the possibility to study interfacial magnetism and interfacial spin polarization. The application potential of such effect in the field of sensors and non volatile memory (MRAM) was also a driven locomotive for the research on MTJs. Replacing the insulating layer by semiconductor materials is a work which has begun recently and where the motivation draws together different fields of spintronic. One of them is in a direct continuation of the work on MTJs with the aim of finding new type of barriers with new properties. As an example it is expected to see an increase of the magnetoresistance as a function of the barrier thickness for fully epitaxial Fe/ZnSe/Fe junctions [50]. Another goal is the use of TMR to get some insight on the ferromagnetic/semiconductor interface spin polarization. Achieving highly spin-polarized interfaces represents a first step for the integration of highly spin-polarized injector in semiconductor material. Nevertheless, to date, the magnetoresistance amplitudes [51–53] are still far from those reported with an insulating layer [54–56]. One of the explanations comes from the necessity to lower the growth temperature of the semiconductor to preserve spin-polarized carriers at the interface. This results in the apparition of defects at the interface or in the semiconductor barrier. The role of these defects, which can govern the conduction properties, are generally damageable for the magnetoresistance. We will illustrate this purpose with our recent work on MnAs/GaAs/MnAs junctions where resonant tunneling on an impurity band have been demonstrated thanks to magnetoresistance measurements. Even with a large spin polarization at the MnAs/GaAs interface, small magnetoresistance effects were observed due to resonant tunneling on an asymmetric impurity band of the defects.

Fig. 5 represents the bias dependence of the TMR extracted from R(H) curves. An asymmetric bias dependence is observed, with inversion of the magnetoresistance. We obtain a TMR maximal amplitude of about 2% together with a TMR inversion more or less pronounced at finite bias (from −0.5% to 0%). This behavior was observed for all of the 10 junctions measured on the sample with cross-sectional areas ranging from 8–32 μm^2. Typical characteristics are shown in Fig. 5 for a junction of 16 μm^2. A clear asymmetric bias dependence of the TMR is visible with a maximum positive (negative) TMR occurring at 40 mV (−40 mV) (Fig. 5(b)).

Until now, negative TMR and related asymmetric bias dependence were reported and ascribed to (a) direct tunneling between electrodes of opposite spin polarization related to specific interfacial electronic band structure [46,59]; or (b) resonant tunneling across a single defect in nanometric size junctions [57]. Because of the relative low RS-product (1 kΩ μm^2) of our micron-sized junctions given the barrier height (0.7 eV), estimated from XPS measurement, and thickness (7.5 nm) (corresponding RS-product estimated for direct tunneling is 10^8 Ω μm^2), we ascribe our TMR effects to localized state-assisted tunneling into a broad impurity band. The model include 5 parameters [58], 2 of them, namely the spin polarization and the asymmetry of position, are really unknown, the others which are the characteristic parameters of the band, can be estimated from literature and measurement.

Under this assumption, all the TMR bias dependencies were fitted with an additional Lorentzian damping function having a characteristic parameter $V_{1/2} = 60$ meV. Experimental data are well reproduced at all positive and negative bias (solid triangles in Fig. 3(a)) with a MnAs polarization P_L and P_R of 60% at each interface, a defect bandwidth W of 140 ± 10 meV and a mean energy ε_C ranging from −50 to −40 meV. The latter values agree well with characteristics of the deep donor band appearing in LT-grown GaAs epilayers [60]. Such defects are formed from excess arsenic incorporated primarily as arsenic antisites (10^{19}, 10^{20} cm^{-3}) and act as deep donors. Those donors are partly compensated by gallium vacancies (acceptors); as a result the Fermi level is pinned within this deep donor band. This is exactly what we obtain with a Fermi level under the top

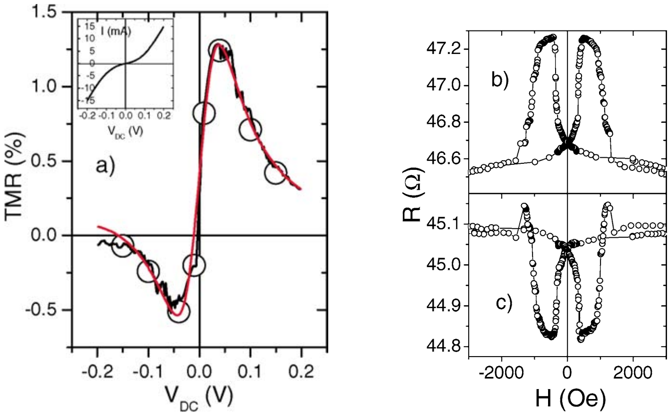

Fig. 5. Data of a 8 μm^2 MnAs/GaAs(7.5 nm)/MnAs tunnel junction recorded at 4 K. (a) *TMR* bias dependence extracted from $I(V)$ (black line) and $R(H)$ (black open symbols) data. The red line represents the calculated value with $P = 60\%$, $\Gamma_L = 6$ meV, $\Gamma_R = 67$ meV, $\epsilon_c = -40$ meV, $W = 140$ meV and $\beta = 0.65$. (b) Field dependence of the junction resistance at 40 mV dc bias. (c) Field dependence of the junction resistance at -40 mV.

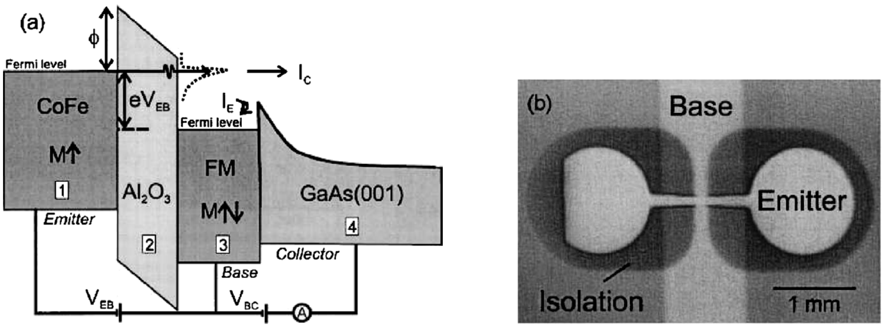

Fig. 6. (a) Schematic energy diagram of the magnetic tunnel transistor (MTT) extract from Ref. [68]. Region 1 is the emitter, region 2 is the Al_2O_3 tunnel barrier, and region 3 is the base. The collector is GaAs (001) substrate (region 4). (b) Photo of the active area of a MTT.

half part of the defect band with the condition $(\varepsilon_F - \varepsilon_C) < W/2$. The defect bandwidth is found to be in the same range as those (150–250 meV) extracted from spectroscopic measurements performed on thick GaAs layers [61,62].

5.1. Hot electrons

Another category of structure which could provide a high efficiency of injected spin-polarized electrons in a semiconductor, is the hot electron transistor. The term 'transistor' refers more to the 3 terminal configuration of the device than to the function of a transistor. The interest of manipulating hot (non thermalized) electrons is, on the one hand, the study of spin-dependent electron transport above the Fermi level [63–65] and, on the other hand, to provide a high efficient source of spin-polarized current highly sensitive to magnetic field. Following pioneering work on hot electron transistor where the base was an active CPP GMR element [66,67], a more recent version uses a TMR element as represented on Fig. 6. In a magnetic tunnel transistor (MTT), spin-polarized electrons are injected from a ferromagnetic emitter across a tunnel barrier into a FM base layer. By changing the bias voltage across the tunnel barrier (V_{EB}) the energy of the injected electrons can be varied. When the electron energy exceeds the Schottky barrier height (Φ_S) at the metal/semiconductor interface, a collector current I_C is measured. I_C represents electrons that are transported across the base layer and the base/collector interface. The injected spin-polarized electron current is further spin filtered by spin dependent scattering in the FM base. Thus I_C depends critically on the relative orientation of the base and emitter magnetic moments, as described by $M_C = (I_{C,P} - I_{C,AP})/I_{C,AP}$ where $I_{C,P}$ and $I_{C,AP}$ are the collector current for parallel and antiparallel alignment of these moments. I_C also depends on the conduction band structure of the semiconductor substrate.

In a version where the ferromagnetic base was replaced by a spin valve element, large M_C as high as 3400% have been demonstrate at small emitter/base bias voltages ($V_E B$) [69]. For practical applications, another interesting feature is a large increase of the collector current (in the order of μA) compared to the CPP GMR spin valve previous version of the transistor

(SVT) where the collector current was in the order of the nA [70]. Finally, one further step was to test the efficiency of the MTT as a source of spin-polarized current into a semiconductor. That the experiment which was performed by Jiang and co-worker [71] by using InGaAs quantum wells and optical detection of the light polarization as described in the Section 3 of this article. Preliminary result have shown an electroluminescent polarization of 10% where the low level of polarization is mostly attributed to a lost of polarization into the quantum well before the electrons-holes recombination process.

6. Conclusion

We have shown that major achievement have been realized in the field of spintronic with semiconductors. The fundamental knowledge of the ferromagnetic-semiconductor interface has been improved and injection of spin-polarized current into III–V semiconductors has been demonstrated. In addition, it has been shown that diluted magnetic semiconductor as GaMnAs can represent another source of spin-polarized carriers. Nevertheless, two points need to be addressed to impose this type of material as a serious alternative to transition metals, for example. First, a Curie temperature above the room temperature has to be reached. Second, a way to inject spin-polarized electrons rather than holes to avoid fast spin relaxation of holes need to be developed. These two points are activating an intense research effort on the fabrication of new DMS type materials.

To make progress in the field of spintronic with semiconductors, the next step should be the demonstration of a complete electrical device including injection and detection of spin-polarized current in various semiconductors. This step is a prerequisite to investigating the expected wealth of the field. It should also constitute the base for the three terminal devices, with manipulation of the spin current. Combining spin injection and detection with the size reduction of semiconductor materials should permit the start of the study of resonant tunneling on discrete energy levels [72]. New magnetoresistance effect, such as the magneto-coulomb blockade, can be anticipated if charge and spin control can be achieved in nanostructures.

References

[1] M.N. Baibich, et al., Phys. Rev. Lett. 61 (1988) 2472.
[2] S.S.P. Parkin, et al., Proc. IEEE 91 (2003) 661–680.
[3] N. F Mott, Proc. R. Soc. London Ser. A 153 (1936) 699–717.
[4] N.F. Mott, Proc. R. Soc. London Ser. A 153 (1936) 368–382.
[5] I.A. Campbell, A. Fert, Transport properties of ferromagnets, in: Ferromagnetic Materials: A Handbook on the Properties of Magnetically Ordered Substances, vol. 3, North-Holland, 1982, p. 747.
[6] S.A. Wolf, et al., Science 294 (2001) 1488.
[7] S. Datta, B. Das, Appl. Phys. Lett. 56 (1990) 665.
[8] H. Ohno, et al., Phys. Rev. Lett. 68 (1992) 2664.
[9] H. Ohno, et al., Appl. Phys. Lett. 69 (1996) 363.
[10] I. Zutic, J. Fabian, S. Das Sarma, Rev. Mod. Phys. (2004) 76.
[11] G. Schmidt, et al., Phys. Rev. B 62 (2000) 4790.
[12] E. Rashba, Phys. Rev. B 62 (2000) R46267.
[13] A. Fert, H. Jaffrès, Phys. Rev. B 64 (2001) 184420;
J. Kikkawa, D. Awschalom, Phys. Rev. Lett. 80 (1998) 4313.
[14] Z.G. Yu, M.E. Flatte, Phys. Rev. B 66 (R) (2002) 201202.
[15] M. Jullière, Phys. Lett. A 54 (1975) 225.
[16] R. Landauer, IBM J. Res. Develop. 1 (1957) 223.
[17] J. Bardeen, Phys. Rev. Lett. 6 (1961) 57.
[18] J.-M. George, et al., Mol. Phys. Rep. 40 (2004) 23.
[19] C. Weisbush, B. Vinter, Quantum Semiconductor Structures – Fundamentals and Applications, Academic, Boston, 1991.
[20] R. Fiederling, et al., Nature 402 (1999) 787.
[21] B.T. Jonker, et al., Phys. Rev. B 62 (2000) 8180.
[22] A.T. Hanbicki, et al., Appl. Phys. Lett. 80 (2002) 1240.
[23] H.J. Zhu, et al., Phys. Rev. Lett. 87 (2001) 016601.
[24] B.L. Liu, et al., Physica E 17 (2003) 358.
[25] X.Y. Dong, et al., Appl. Phys. Lett. 86 (2005) 102107.
[26] M. Ramsteiner, et al., Phys. Rev. B 66 (2002) 081304.
[27] V.F. Motsnyi, et al., Phys. Rev. B 68 (2003) 245319.
[28] X. Jiang, et al., Phys. Rev. Lett. 94 (2005) 056601.
[29] P. Van Dorpe, et al., Appl. Phys. Lett. 84 (2004) 3495.
[30] J. Seufert, et al., Phys. Rev. B 69 (2004) 035311.
[31] C.H. Li, et al., Appl. Phys. Lett. 86 (2005) 132503.

[32] D. Ferrand, et al., Phys. Rev. B 63 (2001) 085201.
[33] A. Haury, et al., Phys. Rev. Lett. 79 (1997) 511.
[34] Y.D. Park, et al., Science 295 (2002) 651.
[35] S.J. Pearton, et al., Semicond. Sci. Technol. 19 (2004) R59.
[36] W. Prellier, et al., J. Phys.: Condens. Matter 15 (2003) R1583.
[37] T. Dietl, Phys. Rev. B 63 (2001) 195205.
[38] H. Ohno, et al., Nature 408 (2000) 944.
[39] H. Boukari, et al., Phys. Rev. Lett. 88 (2002) 207204.
[40] H. Ohno, et al., J. Magn. Magn. Mater. 200 (1999) 110.
[41] M. Tanaka, Y. Higo, Phys. Rev. Lett. 87 (2001) 026602.
[42] R. Mattana, et al., Phys. Rev. Lett. 90 (2003) 166601.
[43] D. Chiba, et al., Phys. Rev. Lett. 93 (2004) 216602.
[44] R. Mattana, et al., Phys. Rev. B 71 (2005) 075206.
[45] J.S. Moodera, et al., Phys. Rev. Lett. 74 (1995) 3273.
[46] J.M. DeTeresa, et al., Science 286 (1999) 507.
[47] D. Chiba, et al., Physica E 21 (2004) 966.
[48] C. Ruster, et al., Phys. Rev. Lett. 94 (2005) 027203.
[49] A. Fert, et al., Europhys. News 34 (2003) 6.
[50] J.M. MacLaren, X.G. Zhang, W.H. Butler, X. Wang, Phys. Rev. B 59 (1999) 5470.
[51] F. Gustavsson, J.M. George, V.H. Etgens, M. Eddrief, Phys. Rev. B 64 (2001) 184422.
[52] X. Jiang, A.F. Panchula, S.S.P. Parkin, Appl. Phys. Lett. 83 (2003) 25.
[53] M. Guth, et al., Appl. Phys. Lett. 78 (2001) 3487.
[54] S.S.P. Parkin, et al., Nature Mater. 3 (2004) 862.
[55] S. Yuasa, et al., Nature Mater. 3 (2004) 868.
[56] D. Wang, C. Nordman, J.M. Daughton, Z. Qian, J. Fink, IEEE Trans. Magn. 40 (2004) 2269–2271.
[57] E.Y. Tsymbal, et al., Phys. Rev. Lett. 90 (2003) 186602.
[58] V. Garcia, et al., Phys. Rev. B 72 (2005) 081303.
[59] C. Tiusan, et al., Phys. Rev. Lett. 93 (2004) 106602.
[60] M. Stellmacher, et al., Semicond. Sci. Technol. 16 (2001) 440.
[61] Y.H. Chen, et al., Appl. Phys. Lett. 72 (1998) 1866.
[62] S. Lodha, et al., J. Appl. Phys. 93 (2003) 2772.
[63] W.H. Rippard, R.A. Burhman, Appl. Phys. Lett. 75 (1999) 1001–1003.
[64] W.H. Rippard, R.A. Burhman, Phys. Rev. Lett. 84 (2000) 971–974.
[65] W.J. Kaiser, L.D. Bell, Phys. Rev. Lett. 60 (1988) 1406–1409.
[66] D.J. Monsma, et al., Phys. Rev. Lett. 74 (1995) 5260.
[67] D.J. Monsma, et al., Science 281 (1998) 407.
[68] S. van Dijken, et al., Phys. Rev. B 66 (2002) 094417.
[69] S. van Dijken, et al., Appl. Phys. Lett. 83 (2003) 951.
[70] A. Kumar, et al., J. Magn. Magn. Mater. 214 (2000) L1–L6.
[71] X. Jiang, et al., Phys. Rev. Lett. 90 (2003) 256603.
[72] A. Slobodskyy, C. Gould, T. Slobodskyy, C.R. Becker, G. Schmidt, L.W. Molenkamp, Phys. Rev. Lett. 90 (2003) 246601.